ACS APPLIED MATERIALS & INTERFACES

www.acsami.org

Research Article

Spatially Segregated MOF Bioreactor Enables Versatile Modular Glycoenzyme Assembly for Hierarchical Glycan Library Construction

Jie Zheng,[#] Han Xu,[#] Bingzhi Li,[#] Muhammad Sohail, Jingjing Bi, Fuming Zhang, Robert J. Linhardt, He Huang,[*] and Xing Zhang[*]

Cite This: *ACS Appl. Mater. Interfaces* 2023, 15, 19807−19816

Read Online

ACCESS | Metrics & More | Article Recommendations | Supporting Information

ABSTRACT: The multienzyme cascade has received growing attention to obtain structurally defined glycans *in vitro*. However, due to poor enzyme stability and low compatibility between glycoenzymes, artificially designed multienzyme pathways to access glycans are often inefficient. Herein, based on the strategy "Modular-Enzymes Assembly by Spatial Segregation" (MASS), we developed a universal immobilization platform to assemble multiple glycoenzymes in compartmentalized MOF particles, inside and outside, significantly reducing the undesired interference and cross-inhibitions. By changing the enzyme modules, a series of glycosyl donor, disaccharides, oligosaccharides, and polysaccharides bearing cofactor regeneration were efficiently prepared. This bioreactor was further successfully applied to the reaction system with high substrate concentration to demonstrate its industrial potential. This robust multienzyme immobilization platform should serve to promote the enzymatic synthesis of more complex glycans.

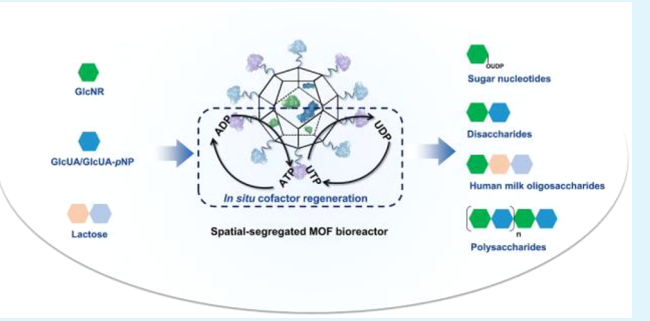

KEYWORDS: *Cascade reaction, metal−organic frameworks, enzyme immobilization, sugar nucleotide, glycan*

INTRODUCTION

Carbohydrates, the most abundant and structurally diverse group of natural products, play an essential role in all living organisms.[1] Because of their potential use in foods, biomedicines, cosmetics materials, and other applications, natural carbohydrates and their non-natural derivatives have emerged as attractive synthetic targets for basic research and in the development of carbohydrate-based drugs.[2,3] Since enzymes are green catalysts with high regio- and stereoselectivity, multienzyme cascades offer an efficient strategy to obtain pure and structurally defined glycans.[4,5] In addition, sugar nucleotides, typically employed by glycosyltransferases as glycosyl donor to monosaccharide acceptors, are critical for the construction of larger glycans. Nevertheless, due to poor enzyme stability and compatibility, the *in vitro* preparation of sugar nucleotides and glycans based on the artificially designed multienzyme pathways is challenging, and often impractical for scale up.[6]

Constructing a universal multiglycoenzyme immobilization platform to simulate *in vivo* natural processes has emerged as a powerful tool to solve this problem,[7,8] as the biomimetic immobilization not only facilitates the enzyme reusability, prolonging shelf life, but also prevents undesired interference and cross-inhibitions that can occur in soluble cascades. Metal−organic frameworks (MOFs), a broad class of porous materials, possess the intriguing physicochemical features of customizable composition, tunable pore aperture, high specific surface area, and biocompatibility. In addition, MOFs, which have balanced rigidity and flexibility that is similar to the cellular environment, are promising to design as a biomimetic microreactor for multiple enzyme cascade.[9,10] However, the current studies about multiple enzyme immobilizations of MOFs have usually been limited to common commercial enzymes (e.g., lipases, peroxidases, glucose oxidases, etc.) catalyzing very simple reactions and have not been extended to the synthesis of complex carbohydrates.[11−13] This may be attributed to the relative instability of glycoenzymes and limitation of a carrier's structure on the transfer of macromolecular sugar substrates.[14]

It is widely known that *in vivo* biosynthesis of glycan or glycoconjugate typically involves stepwise assembly, and the glycan intermediates transport between distinct organelles, such as endoplasmic reticulum and Golgi apparatus.[15] Inspired by this phenomenon, we first developed a strategy "Modular-Enzyme Assembly by Spatial Segregation" (MASS) to

Received: December 7, 2022
Accepted: March 10, 2023
Published: March 17, 2023

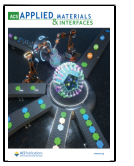

Scheme 1. (a) Illustration of the Multienzyme Immobilization Strategy. (b) Immobilized Multienzyme Systems Applied to Glycosyl Donor, Disaccharides, Oligosaccharides, and Polysaccharides Synthesis

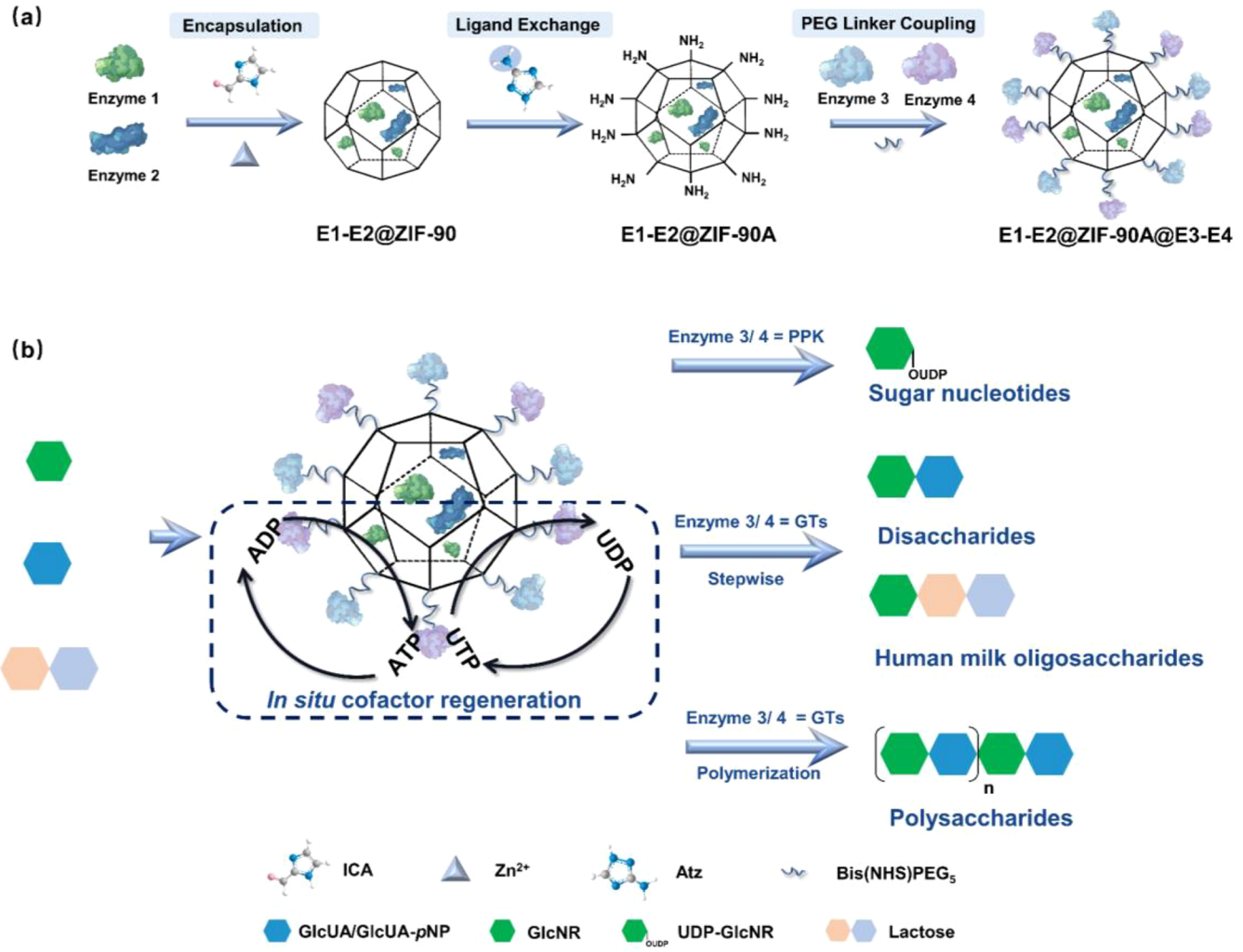

construct an inside and outside compartmentalization-channeling reactor, which allows the different glycoenzyme modules to physically assemble on a single MOFs particle for operating continuous biocatalytic reactions in one-pot. By changing the enzyme module assembly fashion (nine enzymes involved in this work), a series of glycosyl donor, disaccharides, oligosaccharides, and polysaccharides bearing cofactor regeneration were successfully prepared in efficient yields compared to free enzymes cascade.

EXPERIMENTAL SECTION

Synthesis of E1-E2@ZIF-90 via Biomimetic Mineralization. The synthesis of E1-E2@ZIF-90 biocomposite was carried out using a final metal to ligand ratio Zn^{2+} ICA = 1:6, the final concentration were 40 mM and 240 mM. The stock solution of the corresponding precursors $Zn(NO_3)_2{\cdot}6H_2O$ (320 mM), ICA (400 mM), and enzymes (E1 NahK 7.3 mg/mL, E2 GlmU 7.3 mg/mL) were prepared in DI water at room temperature, respectively (Table S1). The two enzymes were first mixed in equal volumes. 1.2 mL ICA in aqueous solution was premixed with 0.55 mL enzyme solution, and then 0.25 mL Zn^{2+} stock solution was added to this mixture to afford E1-E2@ZIF-90, keeping the solution at 4 °C for 24 h. Afterward, the solids were collected by centrifugation and washed three times with water.

Synthesis of E1-E2@ZIF-90A via a Postsynthetic Ligand Exchange Method. The solids E1-E2@ZIF-90 were suspended in 10 mL DI water. Amino-1*H*-1,2,4-triazole (Atz, 0.5 mmol) was added to the E1-E2@ZIF-90 suspension. The postsynthetic ligand exchange reaction was performed at 45 °C for 1 h. Then, the product E1-E2@ZIF-90A was taken out and washed three times with DI water. Finally, the resultant was suspended in 2 mL DI water.

Synthesis of E1-E2@ZIF-90@E3 and E1-E2@ZIF-90@E3-E4 Bioreactors. Linker bisNHS$(PEG)_5$ (0.1 mM) was prepared in pH 7.5 Tris-HCl. Prepare corresponding enzymes E3 (2 mg/mL) and mixture of E3 and E4 (1 mg/mL, respectively). E1-E2@ZIF-90A suspension was diluted 3 times in DI water prior to use. E1-E2@ZIF-90A, linker bisNHS$(PEG)_5$ (1 mL) and enzyme (1 mL E3 or mixture of E3 and E4) were mixed under bidimensional stirring for 30 min, followed by the removal of unbound bisNHS$(PEG)_5$ and enzymes by centrifugation and washing. Finally, the result was suspended in 1 mL DI water.

Characterizations. The chemical structure of the composite was assessed using a VECTOR-22 Fourier transform infrared (FTIR) spectroscope in the wavenumber range of 400−4000 cm^{-1}. The crystalline structure of the composite was determined using 3 kW X-ray diffractometer (XRD) with a Cu Kα radiation source. The morphology of the composite was analyzed utilizing a Thermo Scientific Apreo 2C high-resolution field emission scanning electron microscope (SEM). The specific surface area determination and pore volume were performed by use of Micromeritics ASAP 2460. The zeta potential measurement and dynamic light scattering (DLS) were

https://doi.org/10.1021/acsami.2c22094
ACS Appl. Mater. Interfaces 2023, 15, 19807−19816

carried out by Zetasizer Nano-ZS. The presence and spatial location of FNahK-RGlmU@ZIF-90A@PPK and NahK-GlmU@ZIF-90A@FPPK composites were determined using CLSM technique (Leica TCS SP8 STED). The transmission electron microscope (TEM) observations were performed utilizing a JEOL JEM F200 microscope operated.

Synthesis of UDP-GlcNAc/GalNAc and Their Derivatives. A reaction mixture 200 μL containing Tris-HCl buffer (51.5 mM, pH 7.5), monosaccharides (10 mM), ATP (5 mM), UTP (15 mM), $MgCl_2$ (5 mM), PolyP (15 mM), and NahK-GlmU@ZIF-90A@PPK was incubated at 37 °C for 48 h with shaking (Table S2). Reactions were quenched by adding equal volume ice-cooled cold methanol. Formed sugar nucleotide were detected by HPLC.

Synthesis of the Disaccharides. A 200 μL reaction mixture containing Tris-HCl buffer (51.5 mM, pH 7.5), monosaccharides (10 mM), GlcUA-*p*NP (5 mM), ATP (15 mM), UTP (15 mM), $MgCl_2$ (5 mM), and NahK-GlmU@ZIF-90A@PmHS2 (or NahK-GlmU@ZIF-90A@PmHAS, NahK-GlmU@ZIF-90A@K4CP) was incubated at 37 °C for 48 h with shaking (Tables S3−5). Reactions were quenched by adding equal volume ice-cooled cold methanol, and the resulting disaccharides were detected by HPLC.

High-Titer Enzymatic Synthesis Study. *Sugar Nucleotides.* A reaction mixture 20 mL containing Tris-HCl buffer (100 mM, pH 7.5), monosaccharides (400 mM), ATP (100 mM), UTP (600 mM), $MgCl_2$ (5 mM), PolyP (600 mM), and NahK-GlmU@ZIF-90A@PPK was incubated in metal bath at 37 °C for 60 h with shaking.

Disaccharides. A reaction mixture 20 mL containing Tris-HCl buffer (100 mM, pH 7.5), monosaccharides (200 mM), GlcUA-*p*NP (300 mM), ATP (100 mM), UTP (300 mM), $MgCl_2$ (5 mM), PolyP (450 mM), and NahK-GlmU@ZIF-90A@PmHS2-PPK (or NahK-GlmU@ZIF-90A@PmHAS-PPK) was incubated at 37 °C for 60 h with shaking.

Synthesis of Hyaluronic Acid Polysaccharide and Derivatives. A reaction mixture 200 μL containing Tris-HCl buffer (44 mM, pH 7.5), monosaccharides (10 mM), GlcUA-*p*NP (10 mM), UDP-GlcUA (10 mM), ATP (15 mM), UTP (15 mM), $MgCl_2$ (5 mM), and NahK-GlmU@ZIF-90A@PmHAS was incubated in metal bath at 37 °C for 48 h with shaking (Table S6). Polyacrylamide gel electrophoresis (PAGE) was used to detect sugar chains. Phenol red dye was added to the sample for visualization of the ion front during electrophoresis. A 10 μL aliquot of each sample was analyzed on a 15% gel ran in tris-glycine buffer. The gel was visualized by Alcian blue staining (0.5% w/v Alcian blue 8GX and 2% v/v aqueous acetic acid).

Synthesis of Human Milk Oligosaccharides. *LNT II.* A 200 μL reaction mixture containing Tris-HCl buffer (49 mM, pH 7.5), GlcNAc (10 mM), ATP (15 mM), UTP (15 mM), $MgCl_2$ (5 mM), lactose (10 mM), and NahK-GlmU@ZIF-90A@NmLgtA was incubated in an incubator shaker at 37 °C for around 48 h with shaking and stopped by boiling the solution for 5 min (Table S7).

LNT. A 200 μL reaction mixture containing Tris-HCl buffer (44 mM, pH 7.5), GlcNAc (10 mM), ATP (15 mM), UTP (15 mM), $MgCl_2$ (5 mM), lactose (10 mM), UDP-Gal (10 mM), and NahK-GlmU@ZIF-90A@NmLgtA-Cvβ3GalT was incubated in an incubator shaker at 37 °C for 48 h with shaking and stopped by boiling the solution for 5 min (Table S8).

Sia-LNT II. A reaction mixture 200 μL containing Tris-HCl buffer (44 mM, pH 7.5) containing GlcNAc (10 mM), ATP (15 mM), UTP (15 mM), $MgCl_2$ (5 mM), lactose (10 mM), CMP-Neu5Ac (10 mM), and NahK-GlmU@ZIF-90A@NmLgtA-Pd2,6ST was incubated in an incubator shaker at 37 °C for 48 h with shaking and stopped by boiling the solution for 5 min (Table S9).

Molecular Docking Study. A Lamarckian genetic algorithm in AutoDock 4.2 (Molecular Graphics Laboratory, La Jolla, CA, USA) was applied for the molecular docking study. The structural information of NahK and GlmU was obtained by Protein Data Bank.

RESULTS AND DISCUSSION

Fabrication and Characterization of E1-E2@ZIF-90A@E3-E4 Bioreactors. As illustrated in Scheme 1, enzyme 1 (E1) and enzyme 2 (E2) were first coembedded within zeolitic imidazolate framework (ZIF-90) via mineralization, followed by a postsynthetic ligand exchange strategy to functionalize primary amine groups on the external surface of the composite to form E1-E2@ZIF-90A by introducing 3-amino-1,2,4-triazole (Atz). The resulting composite can be further coupled with enzyme 3 and 4 (E3 and E4) by cross-linker bis(NHS)PEG_5 via amino-succinimide chemistry to construct the multi-glycoenzyme cascade bioreactor E1-E2@ZIF-90A@E3-E4. It is worth noting that the three enzymes cascade bioreactor can also be prepared using the same procedure. ICA/Zn^{2+} ratio, the amount of enzymes and bis(NHS)PEG_5, time, and temperature of ligand exchange would affect the catalytic activity of the bioreactor. Sugar nucleotides are important glycosyl donors in glycan biosynthesis and metabolism, and the MASS strategy was first applied to a multienzyme cascade system of sugar nucleotide synthesis and to construct a NahK-GlmU@ZIF-90A@PPK reactor as model bioreactor. The E1 *N*-acetylhexosamine 1-kinase (NahK) and E2 *N*-acetylglucosamine 1-phosphate uridyltransferase (GlmU), applying to glycosyl donor synthesis, were encapsulated within ZIF-90 through mineralization with the encapsulation efficiency of 100%. The E3 polyphosphate kinase (PPK), specializing in cofactor regeneration, was immobilized outside of composite and showed a high ligation efficiency of 95% (Figure S1 and Table S10).

As revealed by scanning electron microscopy (SEM) images (Figure 1a), the NahK-GlmU@ZIF-90A@PPK displayed a similar morphology to the pure ZIF-90 crystals and presented a rhombic dodecahedral morphology with the particle sizes of 2−5 μm (Figure S2). TEM-EDS analysis was presented in Figure 1b, showing the existence of C, N, O, S, P, and Zn elements in the NahK-GlmU@ZIF-90A@PPK. The X-ray diffraction patterns of the composites were in good agreement with simulated patterns of pure ZIF-90. The diffraction peaks in the XRD patterns of those composites have shown lower intensity in comparison with ZIF-90 single crystal which indicated that the immobilization process changed the crystal

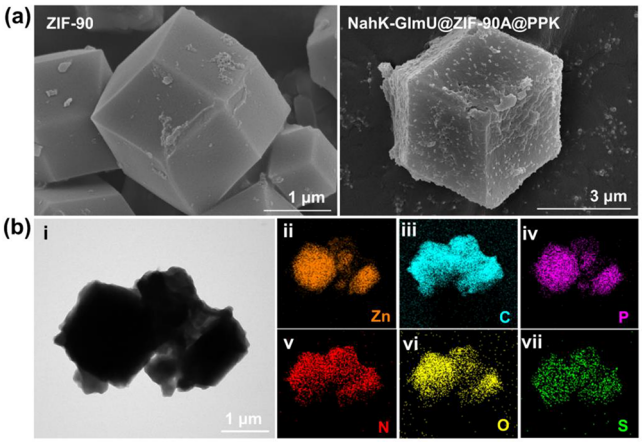

Figure 1. (a) SEM images of ZIF-90 and NahK-GlmU@ZIF-90A@PPK. (b) TEM-EDS elemental mapping images of NahK-GlmU@ZIF-90A@PPK.

https://doi.org/10.1021/acsami.2c22094
ACS Appl. Mater. Interfaces 2023, 15, 19807−19816

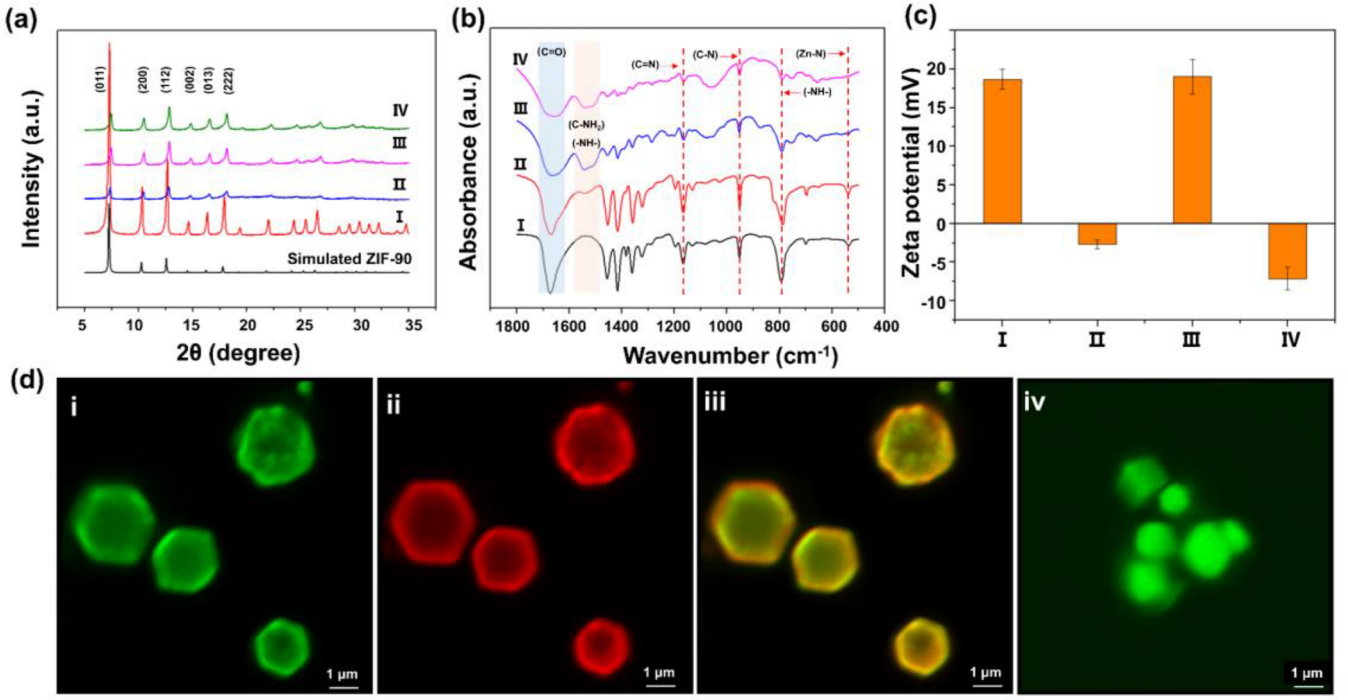

Figure 2. (a) XRD pattern, (b) FTIR spectra, (c) zeta potential value of ZIF-90 (I), NahK-GlmU@ZIF-90 (II), NahK-GlmU@ZIF-90A (III), and NahK-GlmU@ZIF-90A@PPK (IV); values represent the mean ± SD of three independent experiments (n = 3). (d) CLSM images of FNahK-RGlmU@ZIF-90A@PPK and NahK-GlmU@ZIF-90A@FPPK: FITC-labeled NahK (i), RITC-labeled GlmU (ii), a merged image (iii), and FITC-labeled PPK (iv).

phase, and also confirmed that enzymes were successfully encapsulated into ZIF-90 (Figure 2a).[16,17]

The samples were next analyzed by Fourier transform infrared spectroscopy (FTIR) (Figure. 2b). The peaks at 1170 cm^{-1} (C═N), 951 cm^{-1} (C−N), and 789 cm^{-1} (−NH−) were attributed to characteristic absorption of imidazole moieties of ZIF-90.[18] Furthermore, the peaks at 1670 cm^{-1} could be ascribed to the C═O stretching vibrations of aldehyde groups. The characteristic peaks have been reported at 1540 and 1660 cm^{-1} corresponded to the stretching vibrations of the protein-specific amide II bonds (−NH−) and amide I bonds (C═O), respectively.[17] The signal peak of C-NH_2 at 1580 cm^{-1} indicated that ZIF-90 was successfully amine-functionalized.[19] Besides, zeta potential values were also investigated to verify the microcomposite synthetic process. As shown in Figure 2c, the zeta potential value of NahK-GlmU@ZIF-90 diverted from 18.7 mV to −2.7 mV, indicating that the negatively charged enzymes NahK and GlmU were successfully encapsulated. The postsynthetic ligand exchange was confirmed by a shift in the zeta potential value of NahK-GlmU@ZIF-90A from −2.7 mV to 19.0 mV due to the presence of positively charged $-NH_3^+$ on Atz, and that of NahK-GlmU@ZIF-90A@PPK changed to −7.3 mV, indicating the successful PPK immobilization on the NahK-GlmU@ZIF-90A surface.

The immobilization of the three enzymes in the ZIF-90 particle was confirmed by fluorescence confocal microscopy imaging (Figure 2d and Figure S3). Excitation of the FNahK-RGlmU@ZIF-90A@PPK at 488 nm yielded the green fluorescence of the fluorescein isothiocyanate (FITC)-labeled NahK (FNahK) and at 543 nm yielded red fluorescence of the Rhodamine B isothiocyanate (RITC)-functionalized GlmU (RGlmU). The images indicated that the two enzymes were confined in the nanoparticle. The conjugation of the enzyme on the surface of ZIF-90 by PEG linker was confirmed by FITC-labeled PPK (FPPK). The green fluorescence of NahK-GlmU@ZIF-90A@FPPK could be observed under confocal laser scanning microscopy, indicating that PPK was uniformly distributed on ZIF-90.

Synthesis of UDP-GlcNAc/GalNAc and Their Derivatives. The biocatalytic reactor NahK-GlmU@ZIF-90A@PPK was applied to sugar nucleotide synthesis, using GlcNAc as the model substrate (Figure 3 and Figure S4). It is worth noting that NahK-GlmU@ZIF-90A@PPK showed ∼1.4-fold (UDP-GlcNAc **a1**) catalytic activity improvement than homogeneous diffusional mixture of free enzymes (free NahK, GlmU, and PPK). Similarly, UDP-GalNAc **a7** was also efficiently synthesized from GalNAc by NahK-GlmU@ZIF-90A@PPK, and the conversion rate was also higher than free enzymes system (∼4-fold). Furthermore, we evaluated the catalytic activity of unassembled enzyme-loaded ZIF-90 (NahK@ZIF-90, GlmU@ZIF-90, and ZIF-90A@PPK) and three enzymes coencapsulated inside ZIF-90 particle (NahK-GlmU-PPK@ZIF-90) (Figures S5−6). It is discovered that NahK-GlmU@ZIF-90A@PPK exhibited much higher catalytic efficiency than the other two immobilization systems.

We further explored a series of unnatural monosaccharides to investigate the substrate specificity of enzymes in the developed bioreactor NahK-GlmU@ZIF-90A@PPK. It is reported that free NahK-GlmU can recognize a few GlcNAc and GalNAc derivatives bearing C2 modifications.[20,21] Therefore, NahK-GlmU@ZIF-90A@PPK was applied to a series of derivatives, including *N*-trifluoroacetyl (GlcNTFA and GalNTFA), *N*-azidoacetyl (GlcNAz and GalNAz), *N*-butanoyl (GlcNBu and GalNBu), *N*-propionyl (GlcNPr and GalNPr) and bulky *N*-benzoyl (GlcNBz). The molecular diameter of ATP, UTP, and GlcNBz, the largest substrate among

https://doi.org/10.1021/acsami.2c22094
ACS Appl. Mater. Interfaces 2023, 15, 19807−19816

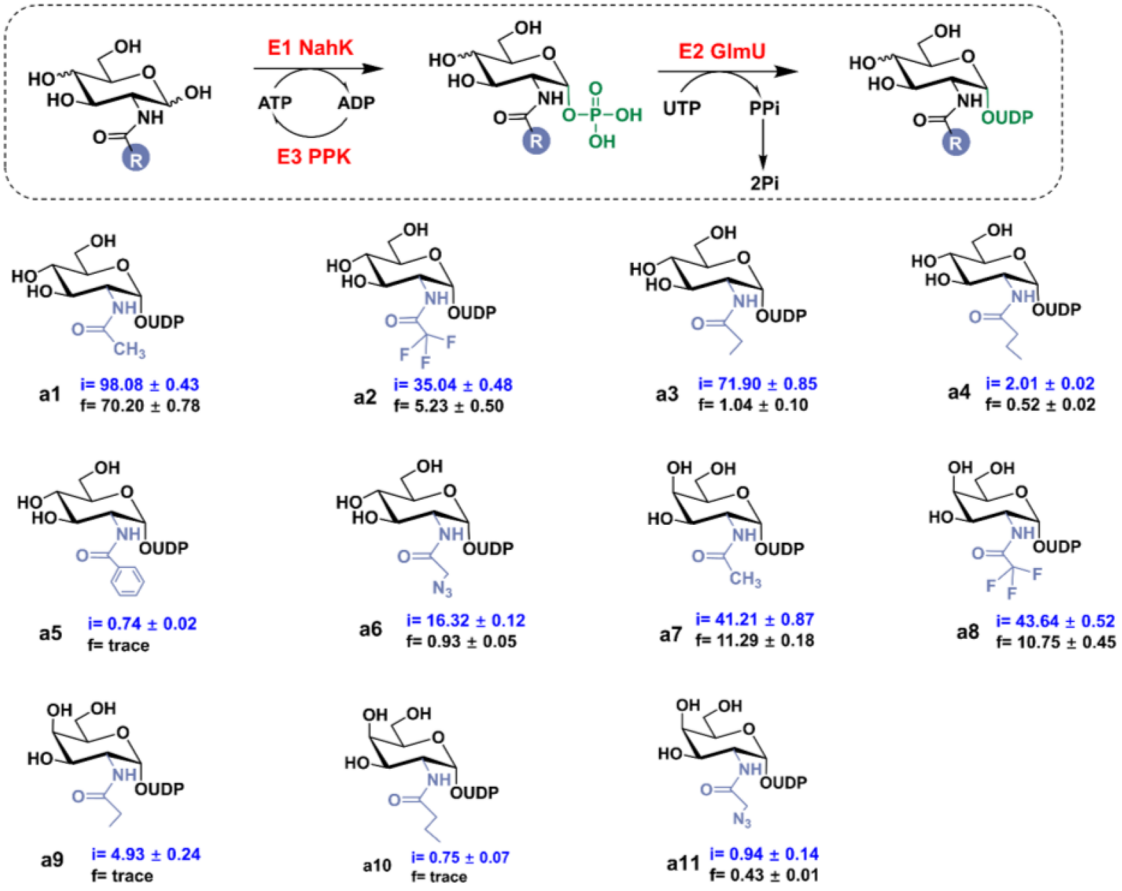

Figure 3. Synthesis of UDP-GlcNAc, UDP-GalNAc, and their derivatives by NahK-GlmU@ZIF-90A@PPK bioreactor. Conversion rate (%) of immobilized multienzymes system (i) and free enzymes system (f). Values represent the mean ± SD of three independent experiments (n = 3). Mass and NMR spectra were shown in Figures S21−29 and Figures S32−35, respectively.

monosaccharides, was calculated by Multiwfn (Figure S7 and Table S11), which was smaller than the pore size of NahK-GlmU@ZIF-90A@PPK (Figure S8), allowing the substrate/product transportation and ensuring the mass-transfer efficiency. All nine derivatives were accepted by NahK-GlmU@ZIF-90A@PPK (Table S12), showing that enzyme immobilization did not adversely impact the substrate specificity. Although the conversion rate of UDP-GlcNAc/GalNAc derivatives are lower than authentic sugar due to the intrinsic properties of enzymes, the developed immobilization platform indeed exhibited significant enhancements in catalytic efficiencies compared with soluble free enzyme cascades. These unnatural UDP-sugars are beneficial to prepare functional carbohydrates. For example, GlcNTFA/GalNTFA incorporated into glycans could be conveniently subjected to deacetylation and sulfation to obtain sulfated saccharides.[22] UDP-GlcNAz and UDP-GalNAz, bearing azido groups, are useful probes in glycobiology by bio-orthogonal labeling reactions.[23,24]

Molecular Docking Study. A molecular docking study concerning enzyme to substrate binding energy was conducted to further verify the critical role of ZIF-90 in the catalysis. Considering the complexity of the entire structure of the frameworks, we proposed a simplified ZIF-90 model, imidazole-2-carboxylaldehyde monomer (Figures S9−13), to simulate the composite as previously reported.[25] The hydroxyl group of anomeric carbon atom (C1-OH) of acceptor substrate GlcNAc was first deprotonated by the amino acid residues Asp208 and Asp228 of NahK to attack the γ-P atom of ATP to afford GlcNAc-1-P. The residues Thr82 and Lys25 of GlmU and the Mg^{2+} can stabilize and precisely orient the negatively charged GlcNAc-1-P for the nucleotidyl-transfer reaction to obtain UDP-GlcNAc (Figure 4a). The binding energy between NahK and GlcNAc, labeled as NahK-GlcNAc, was −5.11 kJ mol^{-1}, while after the introduction of ZIF-90, the corresponding energy of the composite, labeled as [NahK-(ZIF-90)]-(GlcNAc), dropped to −5.24 kJ mol^{-1} (Figure 4b). The binding energy between GlmU and GlcNAc-1-P, labeled as GlmU-(GlcNAc-1-P), decreased under the influence of ZIF-90, facilitating the catalytic reaction (Figure 4c). Additionally, according to the catalytic mechanism of NahK and GlmU, the anomeric hydroxyl group of GlcNAc was first deprotonated by carboxyl groups of amino acid residues from NahK, and then they sequentially attacked the phosphate groups of ATP and UTP to proceed with phosphorylation and pyrophosphorylation.[26−28] The metal ions from ZIF-90 can accelerate the deprotonation of the carboxyl groups on the amino acid residues of the enzyme to form $-COO^-$, which facilitates the catalytic reaction.[29]

Synthesis of Disaccharides. To further demonstrate the application potential of this MASS strategy, we sought to assemble enzymes modules involved in the sugar nucleotide synthesis and glycosylation to produce oligosaccharides (Figure 5). Here, we chose heparosan synthase PmHS2, a dual action glycosyltransferase from *Pasteurella multocida*, possessing both α1−4-*N*-acetylglucosaminyltransferase and

https://doi.org/10.1021/acsami.2c22094
ACS Appl. Mater. Interfaces 2023, 15, 19807−19816

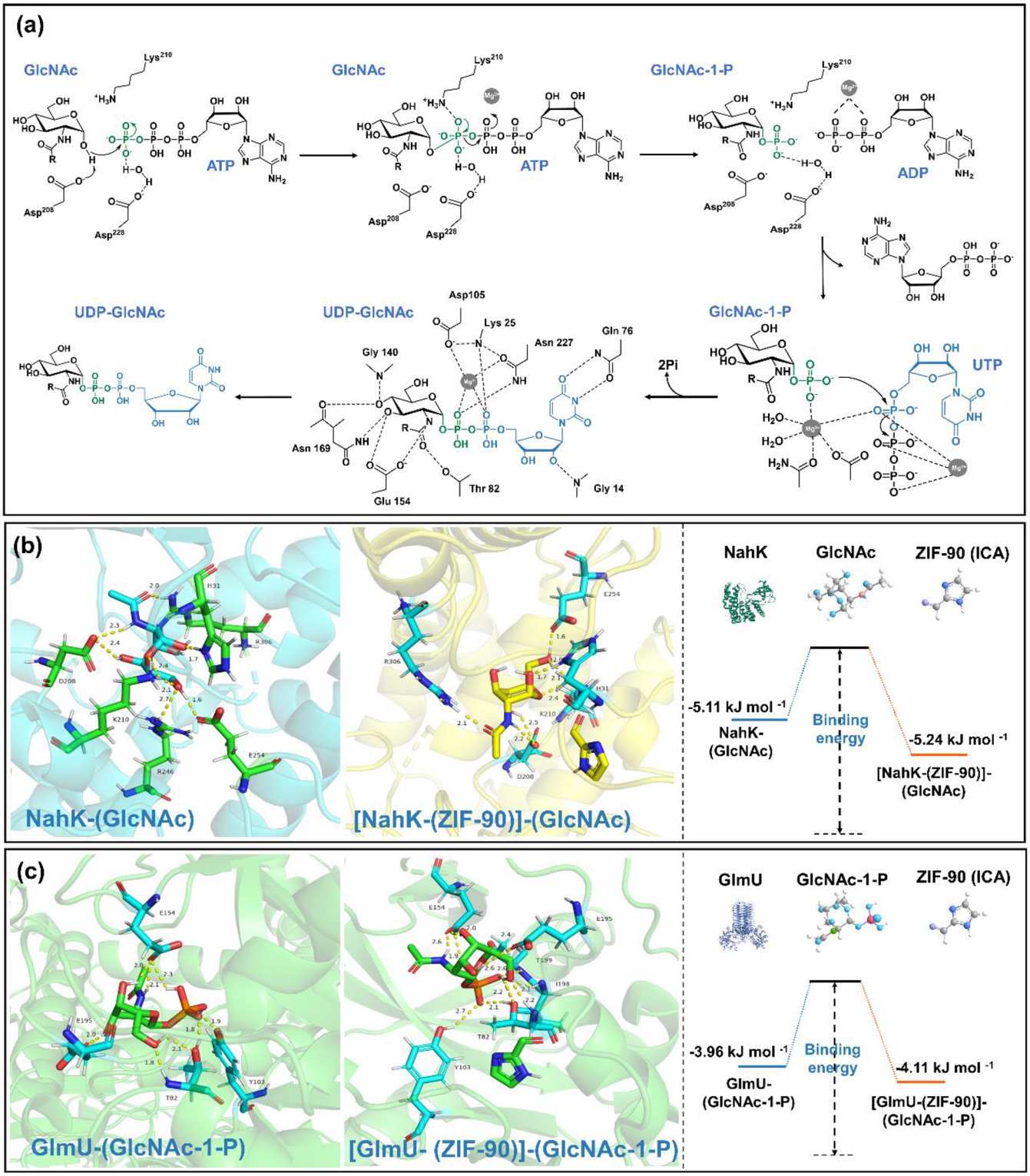

Figure 4. (a) Enzyme catalytic mechanism of UDP-GlcNAc synthesis. Molecular docking and binding energy of (b) NahK-(GlcNAc), [NahK-(ZIF-90)]-(GlcNAc), and (c) GlmU-(GlcNAc-1-P), [GlmU-(ZIF-90)]-(GlcNAc-1-P) as shown by AutoDock.

β1−4-glucuronyltransferase activities,[30] to orderly assemble a multienzymes cascade bioreactor with NahK and GlmU (NahK-GlmU@ZIF-90A@PmHS2) (Figure S14). The glycosyl donor synthesis module (NahK-GlmU) inside ZIF-90 enabled the rapid synthesis of UDP-GlcNR. Subsequently, the resulting nucleotide sugar went through the channeling of the porous ZIF-90 to reach PmHS2 for glycosylation (Table S13).

It is worth noting that GlcNAcα1−4-GlcUA-*p*NP **b1** was obtained with a satisfying conversion rate of 75.3% after three steps, indicating that there is negligible mass transport resistance cross over boundaries between inside and outside of ZIF-90 as well. The molecular diameter of UDP-GlcNBz **a5**, the largest molecule among **a1**−**a11**, was calculated and found smaller than the pore size of ZIF-90 (Figure S15), indicating

https://doi.org/10.1021/acsami.2c22094
ACS Appl. Mater. Interfaces 2023, 15, 19807−19816

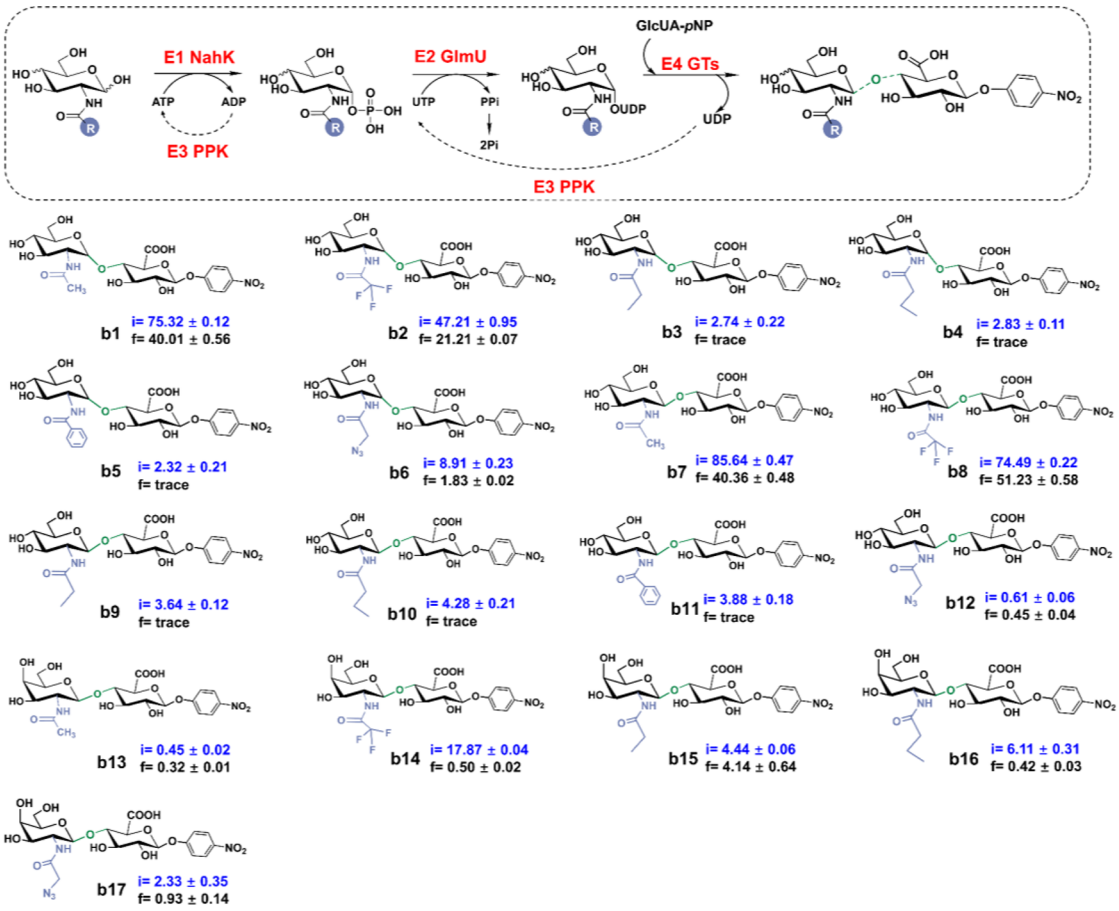

Figure 5. Disaccharide library was prepared by three-enzyme immobilized bioreactors. Conversion rate (%) of (i) immobilized multienzymes system and (f) free enzymes system. Values represent the mean ± SD of three independent experiments (n = 3). Mass and NMR spectra were shown in Figures S30−31 and Figure S36, respectively.

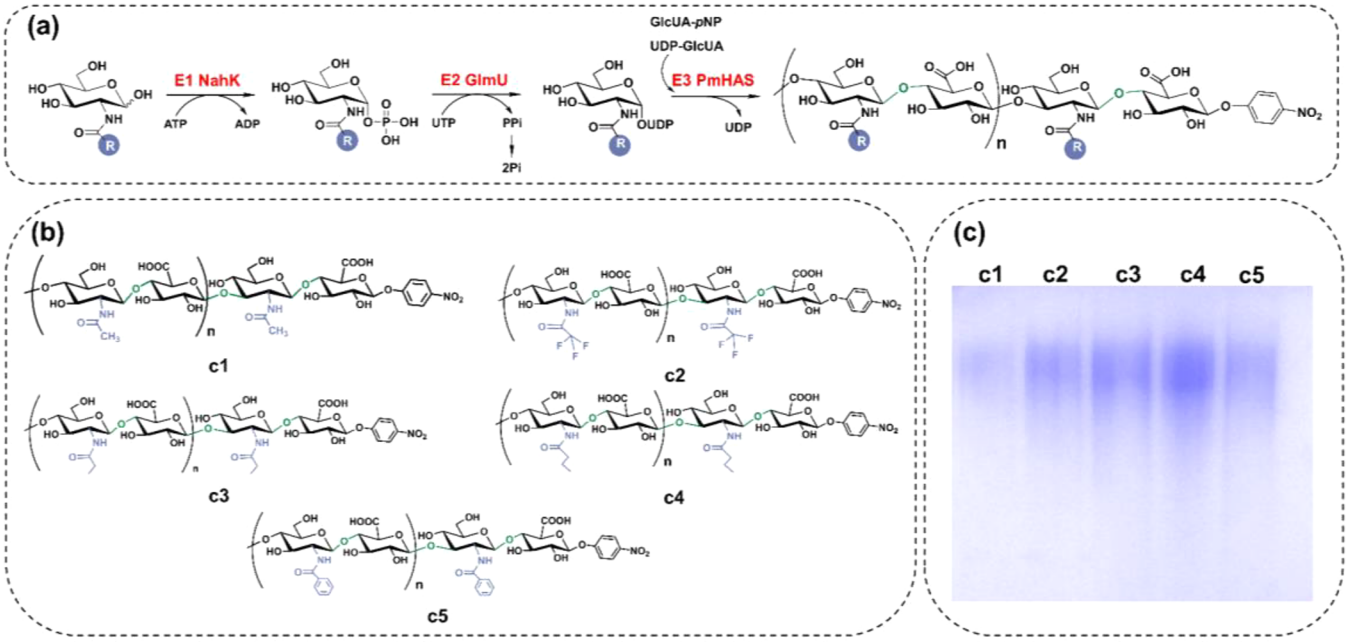

Figure 6. (a) Synthetic scheme, (b) the structures, and (c) PAGE analysis of hyaluronic acid polysaccharide derivatives. NMR spectra was shown in Figure S37.

that the sugar nucleotides **a1**−**a11** can go through the channel and reach the PmHS2 that is immobilized on the surface of ZIF-90 to undergo glycosylation. Disaccharides **b1**−**b6** were successfully prepared via the NahK-GlmU@ZIF-90A@PmHS2

https://doi.org/10.1021/acsami.2c22094
ACS Appl. Mater. Interfaces 2023, 15, 19807−19816

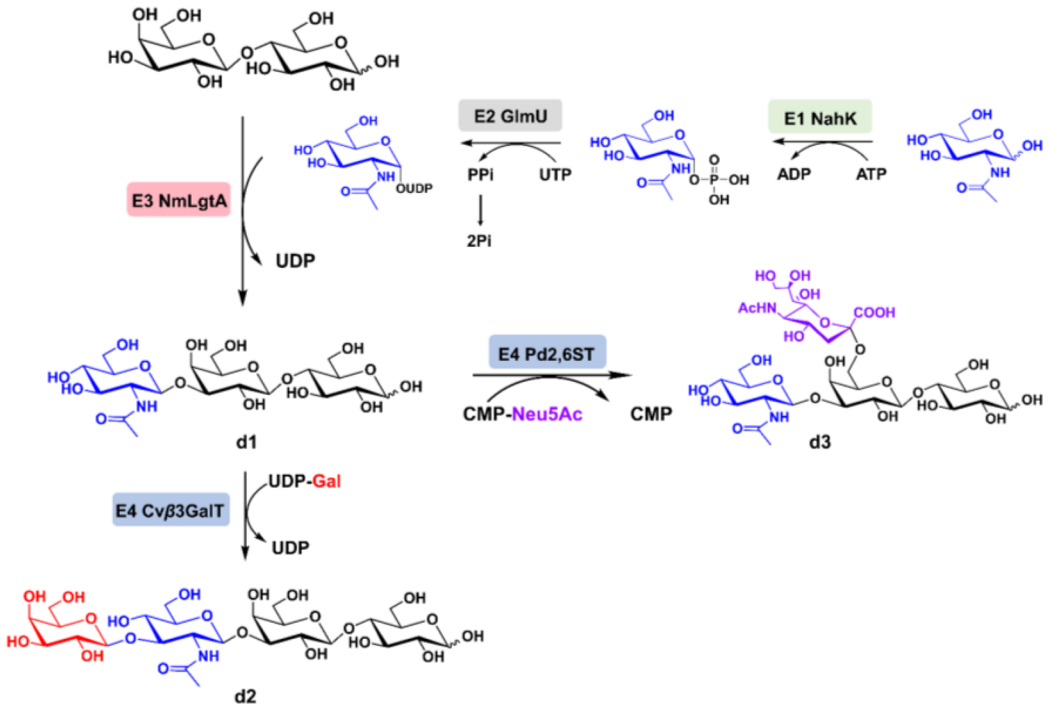

Figure 7. Three human milk oligosaccharides were prepared using corresponding bioreactors. Mass and NMR spectra were shown in Figure S31 and Figures S38−40, respectively.

with enhanced conversion rates compared to soluble enzyme cascades.

By changing the glycosyltransferase module, different kinds of disaccharides can be prepared. *Pasteurella multocida* hyaluronan synthase, PmHAS, and *Escherichia coli* K4 chondroitin synthase K4CP were selected to couple NahK-GlmU to perform cascade reactions to further dig the enzyme broad scope of this immobilization platform.[31,32] Two bioreactors NahK-GlmU@ZIF-90A@PmHAS (Figure S16) and NahK-GlmU@ZIF-90A@K4CP (Figure S17) were successfully employed to obtain hyaluronic acid disaccharides GlcNRβ1−4-GlcUA-*p*NP **b7−b12** and chondroitin disaccharides GalNR β1−4-GlcUA-*p*NP **b13−b17**, respectively. As illustrated in Figure 5, the developed bioreactor showed significantly increased conversion rates compared to soluble enzymes system. Furthermore, it is also discovered that NahK-GlmU@ZIF-90A@PmHAS exhibited much higher catalytic efficiency than the other three immobilization systems (Figures S18−19).

Synthesis of Polysaccharides. This immobilization reactor can be applied to the synthesis of polysaccharides as well. PmHAS, a dual action glycosyltransferase that can catalyze the polymerization of UDP-GlcNAc and UDP-GlcUA to form hyaluronic acid,[33] was employed to construct the NahK-GlmU@ZIF-90A@PmHAS composite (Figure 6a). The resulting hyaluronic acid polysaccharide and derivatives **c1−c5** were analyzed with SDS-PAGE electrophoresis and then stained by alcian blue solution to demonstrate their successful synthesis (Figure 6b,c).

Synthesis of Human Milk Oligosaccharides. Beside the above-mentioned glycosaminoglycan oligosaccharides and polysaccharides, this MASS strategy was applied to other important oligosaccharides preparation, for example, human milk oligosaccharides by changing glycoenzyme modules. Here, we constructed different three-enzyme and four-enzyme cascade systems (Figure 7). First, two nonfucosylated neutral human milk oligosaccharides, GlcNAcβ3Galβ4Glc (LNT II, **d1**) and Galβ3GlcNAcβ3Galβ4Glc (LNT, **d2**), were successfully prepared (Table S14). In the NahK-GlmU@ZIF-90A@NmLgtA system (Figure S20), GlcNAc was first activated by NahK and GlmU, followed by the catalyzation of *Neisseria meningitidis* β1−3-*N*-acetylglucosaminyltransferase (NmLgtA) to form LNT-II in 83% yield. Similarly, LNT was synthesized from lactose in 70% yield by NahK-GlmU@ZIF-90A@NmLgtA-Cvβ3GalT reactor containing NahK, GlmU, NmLgtA, and β1−3-galactosyltransferase Cvβ3GalT. Then, the platform was further employed to immobilize enzymes related to the sialylated HMOs, by the introduction of glycosyltransferase Pd2,6ST to construct NahK-GlmU@ZIF-90A@NmLgtA-Pd2,6ST, and Sia-LNT-II GlcNAcβ3Galβ4-(Siaα6)Glc **d3** was also successfully prepared.

High-Titer Enzymatic Synthesis Study. To investigate the spatially segregated MOF reactor can be practical for high concentration substrate catalysis, UDP-sugar synthesis was chosen as the model reaction and conducted at an elevated scale. With the application of NahK-GlmU@ZIF-90A@PPK can catalyze the substrate, GlcNAc or GalNAc, at the concentration of 400 mM, that is much higher than 200 mM reported in previous studies,[34] UDP-GlcNAc (**a1**) and UDP-GalNAc (**a7**) were synthesized in gram scale. Furthermore, the four-enzyme cascade reactor, including sugar nucleotide synthesis module, glycosylation module, and cofactor regeneration module, was applied to disaccharide synthesis in high titer. When the substrate GlcNAc concentration reached 200 mM, the conversion rate of heparin disaccharide **b1** still reached 70% catalyzed by NahK-GlmU@ZIF-90A@PmHS2-PPK, which is much higher than in the soluble enzyme system due to the inhibitory effect of high concentrations of substrates. Besides, hyaluronic acid disaccharide **b7** exhibited ∼3-fold conversion rates than free enzyme cascades with the

https://doi.org/10.1021/acsami.2c22094
ACS Appl. Mater. Interfaces 2023, 15, 19807−19816

concentration of 200 mM, catalyzed by NahK-GlmU@ZIF-90A@PmHAS-PPK.

CONCLUSIONS

In summary, based on the strategy "Modular-Enzymes Assembly by Spatial Segregation" (MASS), we have successfully developed a universal enzyme immobilization platform that enables flexible assembly of various glycoenzymes modules to achieve the hierarchical glycan library construction with cofactor regeneration. This strategy enabled different enzymes to be held in distinct location of "smart bioreactor"-MOF particle, inside and outside, providing spatial segregation for multistep reactions in one-pot, significantly reducing the undesired interference and cross-inhibitions. Moreover, it exhibited excellent catalytic activity even in a high-concentration substrate system, which is usually difficult to achieve in soluble enzyme cascade reactions, thus, will be beneficial to the large-scale production. To the best of our knowledge, this is the first reported universal multiglycoenzyme immobilization platform and will further promote the enzymatic synthesis of more complex glycans.

ASSOCIATED CONTENT

Supporting Information

The Supporting Information is available free of charge at https://pubs.acs.org/doi/10.1021/acsami.2c22094.

Experimental details; Standard curves of BSA and UDP-GlcNAc; Immobilization efficiency of enzymes; Dynamic light scattering size analysis of biocomposites; Reaction of enzyme's primary amine with fluorescein; The conversion rate of UDP-GlcNAc catalyzed by different immobilization systems; Molecular sizes of substrates; DFT simulation results of pore size distribution; Molecular docking images and analysis results of NahK-(GlcNAc), [NahK-(ZIF-90)]-(GlcNAc), GlmU-(GlcNAc-1-P) and [GlmU-(ZIF-90)]-(GlcNAc-1-P); HPLC spectrum of sugar nucleotides and disaccharides; MS and NMR spectrum/analysis of the synthesized sugar nucleotides, disaccharide, oligosaccharides, and polysaccharide; XRD patterns, zeta potential value, FTIR spectra and SEM image of multienzyme immobilization biocomposites (PDF)

AUTHOR INFORMATION

Corresponding Authors

Xing Zhang − *School of Food Science and Pharmaceutical Engineering, Nanjing Normal University, Nanjing 210023, China;* orcid.org/0000-0002-2699-3448; Email: zhangxing@njnu.edu.cn

He Huang − *College of Biotechnology and Pharmaceutical Engineering, Nanjing Tech University, Nanjing 211816, China; School of Food Science and Pharmaceutical Engineering, Nanjing Normal University, Nanjing 210023, China; State Key Laboratory of Materials-Oriented Chemical Engineering, School of Pharmaceutical Sciences, Nanjing Tech University, Nanjing 210009, China*; Email: huangh@njnu.edu.cn

Authors

Jie Zheng − *College of Biotechnology and Pharmaceutical Engineering, Nanjing Tech University, Nanjing 211816, China; School of Food Science and Pharmaceutical Engineering, Nanjing Normal University, Nanjing 210023, China*

Han Xu − *School of Food Science and Pharmaceutical Engineering, Nanjing Normal University, Nanjing 210023, China*

Bingzhi Li − *School of Food Science and Pharmaceutical Engineering, Nanjing Normal University, Nanjing 210023, China;* orcid.org/0000-0002-5533-2147

Muhammad Sohail − *School of Food Science and Pharmaceutical Engineering, Nanjing Normal University, Nanjing 210023, China*

Jingjing Bi − *Key Laboratory of Green Chemical Media and Reactions, Ministry of Education, School of Chemistry and Chemical Engineering, Henan Normal University, Xinxiang, Henan 453007, China*

Fuming Zhang − *Department of Chemistry and Chemical Biology, Center for Biotechnology and Interdisciplinary Studies, Rensselaer Polytechnic Institute, Troy, New York 12180, United States;* orcid.org/0000-0003-2803-3704

Robert J. Linhardt − *Department of Chemistry and Chemical Biology, Center for Biotechnology and Interdisciplinary Studies, Rensselaer Polytechnic Institute, Troy, New York 12180, United States;* orcid.org/0000-0003-2219-5833

Complete contact information is available at: https://pubs.acs.org/10.1021/acsami.2c22094

Author Contributions

#J. Z., H.X., and B. L. contributed equally.

Notes

The authors declare no competing financial interest.

ACKNOWLEDGMENTS

This work was supported by grants from the National Key Research and Development Program (2021YFC2100100) to X.Z., National Natural Science Foundation, China (22007049) to X.Z., and GlycoMIP a National Science Foundation Materials Innovation Platform funded through Cooperative Agreement DMR-1933525 (to F.Z. and R.J.L.).

REFERENCES

(1) Varki, A. Biological Roles of Glycans. *Glycobiology* **2017**, *27*, 3−49.

(2) Pifferi, C.; Fuentes, R.; Fernandez-Tejada, A. Natural and Synthetic Carbohydrate-Based Vaccine Adjuvants and Their Mechanisms of Action. *Nat. Rev. Chem.* **2021**, *5*, 197−216.

(3) Barile, D.; Rastall, R. A. Human Milk and Related Oligosaccharides as Prebiotics. *Curr. Opin. Biotechnol.* **2013**, *24*, 214−219.

(4) Yu, H.; Chen, X. One-Pot Multienzyme (OPME) Systems for Chemoenzymatic Synthesis of Carbohydrates. *Org. Biomol. Chem.* **2016**, *14*, 2809−2818.

(5) Koeller, K. M.; Wong, C. H. Complex Carbohydrate Synthesis Tools for Glycobiologists: Enzyme-Based Approach and Programmable One-Pot Strategies. *Glycobiology* **2000**, *10*, 1157−1169.

(6) Bandi, C. K.; Agrawal, A.; Chundawat, S. P. S. Carbohydrate-Active Enzyme (CAZyme) Enabled Glycoengineering for a Sweeter Future. *Curr. Opin. Biotechnol.* **2020**, *66*, 283−291.

(7) Zhong, C.; Duic, B.; Bolivar, J. M.; Nidetzky, B. Three-Enzyme Phosphorylase Cascade Immobilized on Solid Support for Biocatalytic Synthesis of Cello-Oligosaccharides. *ChemCatChem.* **2020**, *12*, 1350−1358.

(8) Nahalka, J.; Liu, Z. Y.; Chen, X.; Wang, P. G. Superbeads: Immobilization in "Sweet" Chemistry. *Chem.—Eur. J.* **2003**, *9*, 372−377.

(9) Lian, X.; Fang, Y.; Joseph, E.; Wang, Q.; Li, J.; Banerjee, S.; Lollar, C.; Wang, X.; Zhou, H. C. Enzyme-MOF (Metal-Organic Framework) Composites. *Chem. Soc. Rev.* **2017**, *46*, 3386−3401.
(10) Liang, W.; Wied, P.; Carraro, F.; Sumby, C. J.; Nidetzky, B.; Tsung, C. K.; Falcaro, P.; Doonan, C. J. Metal-Organic Framework-Based Enzyme Biocomposites. *Chem. Rev.* **2021**, *121*, 1077−1129.
(11) Wu, X.; Yue, H.; Zhang, Y.; Gao, X.; Li, X.; Wang, L.; Cao, Y.; Hou, M.; An, H.; Zhang, L.; Li, S.; Ma, J.; Lin, H.; Fu, Y.; Gu, H.; Lou, W.; Wei, W.; Zare, R. N.; Ge, J. Packaging and Delivering Enzymes by Amorphous Metal-Organic Frameworks. *Nat. Commun.* **2019**, *10*, 5156.
(12) Man, T.; Xu, C.; Liu, X. Y.; Li, D.; Tsung, C. K.; Pei, H.; Wan, Y.; Li, L. Hierarchically Encapsulating Enzymes with Multi-Shelled Metal-Organic Frameworks for Tandem Biocatalytic Reactions. *Nat. Commun.* **2022**, *13*, 305.
(13) Nadar, S. S.; Rathod, V. K. Encapsulation of Lipase within Metal-Organic Framework (MOF) with Enhanced Activity Intensified under Ultrasound. *Enzyme Micro. Technol.* **2018**, *108*, 11−20.
(14) Zhao, L.; Ma, Z.; Yin, J.; Shi, G.; Ding, Z. Biological Strategies for Oligo/Polysaccharide Synthesis: Biocatalyst and Microbial Cell Factory. *Carbohyd. Polym.* **2021**, *258*, 117695.
(15) Hang, I.; Lin, C. W.; Grant, O. C.; Fleurkens, S.; Villiger, T. K.; Soos, M.; Morbidelli, M.; Woods, R. J.; Gauss, R.; Aebi, M. Analysis of Site-Specific *N*-Glycan Remodeling in the Endoplasmic Reticulum and the Golgi. *Glycobiology* **2015**, *25*, 1335−1349.
(16) Mahmoodi, N. M.; Abdi, J. Metal-Organic Framework as a Platform of the Enzyme to Prepare Novel Environmentally Friendly Nanobiocatalyst for Degrading Pollutant in Water. *J. Ind. Eng. Chem.* **2019**, *80*, 606−613.
(17) Zou, Y.; Liu, X.; Zhang, H. A Dual Enzyme-Containing Microreactor for Consecutive Digestion Based on Hydrophilic ZIF-90 with Size-Selective Sheltering. *Colloid. Surface. B* **2021**, *197*, 111422.
(18) Fan, C.; Tang, Y.; Wang, H.; Huang, Y.; Xu, F.; Yang, Y.; Huang, Y.; Rong, W.; Lin, Y. ZIF-90 with Biomimetic Zn-N Coordination Structures as an Effective Nanozyme to Mimic Natural Hydrolase. *Nanoscale* **2022**, *14*, 7985−7990.
(19) Liang, J.; Mazur, F.; Tang, C.; Ning, X.; Chandrawati, R.; Liang, K. Peptide-Induced Super-Assembly of Biocatalytic Metal-Organic Frameworks for Programmed Enzyme Cascades. *Chem. Sci.* **2019**, *10*, 7852−7858.
(20) Guan, W.; Cai, L.; Fang, J.; Wu, B.; Wang, P. G. Enzymatic Synthesis of UDP-GlcNAc/UDP-GalNAc Analogs using *N*-Acetylglucosamine 1-Phosphate Uridyltransferase (GlmU). *Chem. Commun.* **2009**, *45*, 6976−6978.
(21) Cai, L.; Guan, W.; Kitaoka, M.; Shen, J.; Xia, C.; Chen, W.; Wang, P. G. A Chemoenzymatic Route to *N*-Acetylglucosamine-1-Phosphate Analogues: Substrate Specificity Investigations of *N*-Acetylhexosamine 1-Kinase. *Chem. Commun.* **2009**, *20*, 2944−2946.
(22) Zhang, X.; Pagadala, V.; Jester, H. M.; Lim, A. M.; Truong Quang, P.; Goulas, A. M. P.; Liu, J.; Linhardt, R. J. Chemoenzymatic Synthesis of Heparan Sulfate and Heparin Oligosaccharides and NMR Analysis: Paving the Way to a Diverse Library for Glycobiologists. *Chem. Sci.* **2017**, *8*, 7932−7940.
(23) Li, X.; Qi, C.; Wei, P.; Huang, L.; Cai, J.; Xu, Z. Efficient Chemoenzymatic Synthesis of Uridine 5-Diphosphate *N*-Acetylglucosamine and Uridine 5-Diphosphate *N*-Trifluoacetyl Glucosamine with Three Recombinant Enzymes. *Prep. Biochem. Biotechnol.* **2017**, *47*, 852−859.
(24) Boyce, M.; Carrico, I. S.; Ganguli, A. S.; Yu, S. H.; Hangauer, M. J.; Hubbard, S. C.; Kohler, J. J.; Bertozzi, C. R. Metabolic Cross-Talk Allows Labeling of *O*-linked *β*-*N*-Acetylglucosamine-Modified Proteins via the *N*-Acetylgalactosamine Salvage Pathway. *Proc. Natl. Acad. Sci. U.S.A.* **2011**, *108*, 3141−3146.
(25) Wang, Q.; Ji, Y.; Zhang, X.; He, H.; Wang, G.; Xu, C.; Lin, L. Boosting the Quantum Yield of Oxygen-Soped g-C_3N_4 via a Metal-Azolate Framework-Enhanced Electron-Donating Strategy for Highly Sensitive Sulfadimethoxine Tracing. *Anal. Chem.* **2022**, *94*, 5682−5689.
(26) Zhao, Y.; She, N.; Ma, Y.; Wang, C.; Cao, Z. A Description of Enzymatic Catalysis in *N*-Acetylhexosamine 1-Kinase: Concerted Mechanism of Two-Magnesium-Ion-Assisted GlcNAc Phosphorylation, Flexibility Behavior of Lid Motif upon Substrate Recognition, and Water-Assisted GlcNAc-1-P Release. *ACS Catal.* **2018**, *8*, 4143−4159.
(27) Mochalkin, I.; Lightle, S.; Zhu, Y.; Ohren, J. F.; Spessard, C.; Chirgadze, N. Y.; Banotai, C.; Melnick, M.; McDowell, L. Characterization of Substrate Binding and Catalysis in the Potential Antibacterial Target *N*-Acetylglucosamine-1-Phosphate Uridyltransferase (GlmU). *Protein Sci.* **2007**, *16*, 2657−2666.
(28) Vithani, N.; Prakash, B.; Nair, N. N. Mechanism of Nucleotidyltransfer Reaction and Role of Mg^{2+} Ion in Sugar Nucleotidyltransferases. *Biophy. J.* **2020**, *119*, 619−627.
(29) Qiao, M.; Ji, Y.; Linhardt, R. J.; Zhang, X.; Huang, H. Fabricating Bimetal Organic Material Capsules with a Commodious Microenvironment and Synergistic Effect for Glycosyltransferase. *ACS Appl. Mater. Interfaces* **2022**, *14*, 26034−26043.
(30) Na, L.; Yu, H.; McArthur, J. B.; Ghosh, T.; Asbell, T.; Chen, X. Engineer *P. multocida* Heparosan Synthase 2 (PmHS2) for Size-Controlled Synthesis of Longer Heparosan Oligosaccharides. *ACS Catal.* **2020**, *10*, 6113−6118.
(31) Gottschalk, J.; Zaun, H.; Eisele, A.; Kuballa, J.; Elling, L. Key Factors for a One-Pot Enzyme Cascade Synthesis of High Molecular Weight Hyaluronic Acid. *Int. J. Mol. Sci.* **2019**, *20*, 5664.
(32) Sobhany, M.; Kakuta, Y.; Sugiura, N.; Kimata, K.; Negishi, M. The Chondroitin Polymerase K4CP and the Molecular Mechanism of Selective Bindings of Donor Substrates to Two Active Sites. *J. Biol. Chem.* **2008**, *283*, 32328−32333.
(33) Jing, W.; DeAngelis, P. L. Analysis of the Two Active Sites of the Hyaluronan Synthase and the Chondroitin Synthase of *Pasteurella Multocida*. *Glycobiology* **2003**, *13*, 661−671.
(34) Li, S.; Wang, S.; Wang, Y.; Qu, J.; Liu, X. W.; Wang, P. G.; Fang, J. Gram-Scale Production of Sugar Nucleotides and Their Derivatives. *Green Chem.* **2021**, *23*, 2628−2633.